

Examining the Binding Affinity of Ribose to YME1L-AAA+ By Competition Titrations

by
Justin West

A thesis presented to the Honors College of Middle Tennessee State University in
partial fulfillment of the requirements for graduation from the University Honors
College

Spring 2021

Thesis Committee:

Dr. Justin Miller, Thesis Director

Dr. Gregory Van Patten, Thesis Committee Chair

Examining the Binding Affinity of Ribose to YME1L-AAA+ By Competition Titrations

by Justin West

APPROVED:

Dr. Justin Miller, Thesis Director
Assistant Professor, Department of Chemistry

Dr. Gregory Van Patten, Thesis Committee Chair
Chair, Department of Chemistry

ACKNOWLEDGEMENTS

I would like to thank my advisor, Dr. Justin Miller for all the time and patience in helping me with this project. I would also like to thank him for all the knowledge he shared with me throughout this two-semester journey. I would like to also thank Mr. Justin Marsee for all his assistance as well throughout the course of this project. I would like to thank my girlfriend, Maddie, for being there for me throughout this project and my overall college experience. I would like to thank her parents Eddie and Judy for all their support. I would like to thank my mother, Angela, and my grandmother, Mary for always being there for me in my times of need.

ABSTRACT

YME1L is an ATP-dependent protease that is involved in both protein quality control and regulation of mitochondrial morphology. One method to detect binding interactions of this protein is through the use of a fluorescently tagged ATP, known as MANT-ATP. ATP is made of a sugar, ribose, a triphosphate group, and a nitrogenous base, adenine. Binding assays that utilize MANT-ATP have been widely used, but sometimes questioned due to possible non-specific binding interactions. The purpose of this study is to look at the difference in interactions between unmodified ATP and the fluorescent analog MANT-ATP. Results show that MANT-ATP binds to not only the active site of the protein, but possibly multiple sites due to non-specific interactions occurring at high MANT-ATP concentration. Furthermore, we look at how ATP binding is affected by the presence of ribose to look at a possible competition effect. These results show that ribose is in fact able to bind to the ATP binding site alone without the presence of adenine or the phosphates.

TABLE OF CONTENTS

AKNOWLEDGEMENTS.....	iii
ABSTRACT.....	iv
LIST OF FIGURES.....	vi
LIST OF ABBREVIATIONS.....	vii
CHAPER 1: INTRODUCTION.....	1
CHAPTER 2: MATERIALS AND METHODS.....	4
CHAPTER 3: RESULTS AND CONCLUSIONS.....	6
WORKS CITED.....	14
APPENDIX A: RIBOSE SPECTRA.....	15

LIST OF FIGURES

FIGURE 1: YME1L Binding Site Structure.....	3
FIGURE 2: Representative MANT-ATP Binding Spectra.....	7
FIGURE 3: Resulting MANT-ATP Binding Parameters	9
FIGURE 4: Representative Binding ATP Emissions Spectra	10
FIGURE 5: Resulting ATP Binding Parameters	11
FIGURE 6: Representative Ribose Binding Spectra.....	12

LIST OF ABBREVIATIONS

AAA+: ATPases associated with various cellular activities

ATP: adenosine triphosphate

MANT-ATP: (2'-(or-3')-O-(N-Methylanthraniloyl) Adenosine 5'-Triphosphate

FRET: fluorescence resonance energy transfer

K_D : dissociation equilibrium constant

YMEIL: yeast mitochondrial escape protein 1

CHAPTER 1: INTRODUCTION

Background

When many people hear the term mitochondria they think of the powerhouse of the cell. This is true, but there is much more importance of the mitochondria to cellular function. Mitochondria are an essential organelle that determines the life and death of eukaryotic cells. They are critical for many cellular processes such as oxidative phosphorylation, the electron transport chain, biomolecular synthesis, calcium homeostasis, and apoptosis (Brambley *et al.* 2019). One important control element that is essential for mitochondrial function is protein quality control. Imbalances in this regulation can be associated with many human diseases such as Alzheimer's, Parkinson's, and Huntington's disease. YME1L is a hexameric AAA+ (ATPases which are associated with various cellular activities) protease in the inner membrane of the mitochondria that controls maintenance of the electron transport chain, protein import, lipid synthesis, and mitochondrial morphology (Puchades *et al.* 2017). Every YME1L subunit contains an ATPase and a peptidase domain, which reside in the intermembrane space (Puchades *et al.* 2017).

In a recent study conducted by Miller *et al.*, MANT-ATP was used to probe nucleotide binding kinetics with the protein YME1L. Non-specific binding is made possible at elevated concentrations of MANT-ATP, likely due to the fluorophore being present. In order to ensure that the binding kinetics study conducted reported only on specific interactions, we conduct this study on the binding parameters of MANT-ATP.

Ribose is a simple sugar and carbohydrate that is produced by the body, particularly the pentose-phosphate pathway. It is important in energy production and is naturally occurring inside cells and the mitochondria. Ribose is an energy producing substrate of the ATP molecule and has a role in intracellular energy transfer (Mahoney, Diane E, et al. 2018). ATP is an organic compound that provides the energy necessary to drive many processes in living cells such as muscle contraction, nerve impulse propagation, and chemical synthesis. ATP is a nucleotide that consists of three main structures: the nitrogenous base adenine, the sugar ribose, and a chain of three phosphate groups. MANT-ATP is a fluorescent analog of ATP and is commonly used in nucleotide-protein interactions.

In Physical and biological systems there can exist different types of interactions, two of which are specific and non-specific interactions. Specific interactions are those that lead to the formation of specific complexes, in this case the ATP-YME1L-AAA+ complex. Non-specific interactions are those of promiscuous interactions between two molecules. These interactions could involve the presence of a chromophore, steric hindrance, or hydrophobic interaction. Specific interactions are critically important for the functioning of the cell and are closely associated with networks of protein-protein interactions (Osmanovic, Rabin. 2016).

For this study we look at how both ATP and MANT-ATP bind to the active site on the mitochondrial ATP-dependent protease, YME1L. Specifically we look to calculate the binding affinities of both ATP and MANT-ATP and see if there is binding to more than one site on the protein, or binding to just the active site (non-specific and specific interaction, respectively). The binding parameters for MANT-ATP will look at

FRET donor and acceptor properties between tryptophan on YME1L and the MANT group on the ATP. FRET describes the energy transferred between two light-sensitive molecules. It is a distance-dependent physical process, and happens via intermolecular long-range dipole-dipole coupling. Figure 1 shows the area of interest on YME1L.

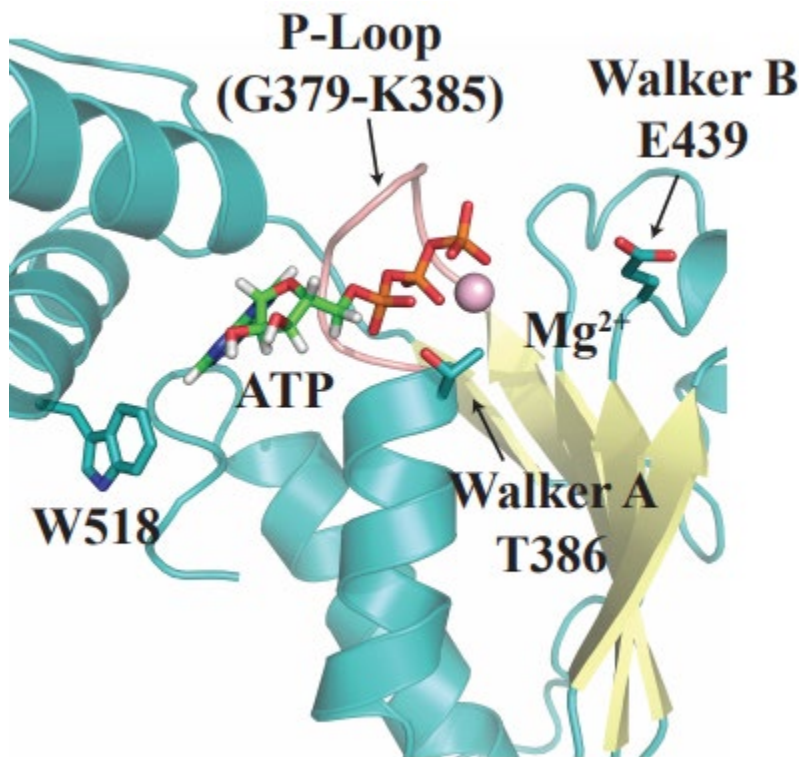


Figure 1. YME1L Binding Site Structure. W518 shows the single tryptophan in the binding site of YME1L. ATP is also pictured to show the specific binding interaction.

We report here that ATP binds to YME1L-AAA+ specifically to the active site with an affinity of 5.3 ± 0.6 micromolar. Although it is possible for ATP to bind nonspecifically, we cannot see it due to the assay design. However, the ATP binding experiment here reports on tryptophan emissions, which we can say is the result of specific binding. In contrast, we report that MANT-ATP binds to YME1L to more than one site, which is likely due to non-specific binding interactions at other sites on the protein, with estimated affinities of 53 ± 10 micromolar and 242 ± 49 micromolar,

respectively. Furthermore, we report that ribose acts as a competitor of ATP with an estimated affinity of 287 ± 45 micromolar. We demonstrate here that ribose can bind to the ATP binding site alone without the normally associated adenine base or phosphate.

CHAPTER 2: MATERIALS AND METHODS

Protein Expression

The YME1L-AAA⁺ overexpression plasmid was synthesized and cloned into the pET-24a(+) vector commercially by Genscript. The YME1L-AAA⁺ domain was prepared as an N-terminal His₆ fusion and overexpressed from the pET24a(+) vector in BL21(DE3) competent cells. The described construct encodes residues 317–584 from human YME1L. The BL21(DE3) cells are a special strain of *E. Coli* that lack key proteases which reduces the degradation of our desired protein. These bacterial cultures were grown in lysogeny broth at 37 °C with shaking until the OD₆₀₀ reached 0.6 absorbance units. At the desired optical density, bacterial cultures were treated with 0.5 mM isopropyl β-D-1- thiogalactopyranoside to induce protein overexpression and incubated at 18 °C for 16 h while being shaken (Miller *et al.* 2020).

Purification

Cell paste was then harvested and resuspended in chilled lysis buffer containing 25 mM Tris (pH 8.3), 500 mM NaCl, 20% glycerol, 10 mM 2- mercaptoethanol, 10 mM imidazole (pH 8), 0.05% (v/v) TWEEN-80, 0.1 mM EDTA, and 1 mM PMSF. Following cell lysis by sonication, the crude lysate was clarified by centrifugation at ~50000g. The clarified lysate was then loaded onto a HisPrep FF 16/10 Ni-NTA column (GE Healthcare, Chicago, IL) previously equilibrated with buffer T300 [10 mM imidazole (pH 8), 50 mM Tris (pH 8.3), 300 mM NaCl, 10% glycerol, and 2 mM 2-

mercaptoethanol]. Following a 2-column volume wash, YME1L-AAA+ was eluted by a linear imidazole concentration gradient from 10 to 500 mM over 8 column volumes. The major elution product was then desalted into H150 buffer [25 mM HEPES (pH 7.5), 150 mM NaCl, 10% glycerol, and 2 mM 2-mercaptoethanol]. The sample was then loaded onto a HiLoad Superdex 200 pg 26/60 preparative size-exclusion column previously equilibrated in H150 buffer. The resulting YME1L-AAA+ was flash-frozen in liquid nitrogen and stored at $-80\text{ }^{\circ}\text{C}$ (Miller et al. 2020). The protein concentration was determined spectrophotometrically in reaction H150 buffer using an extinction coefficient of $1.15 \times 10^4\text{ M}^{-1}\text{ cm}^{-1}$ (ϵ_{280}).

Fluorescence Experiments

Fluorescence experiments were performed using a Hitachi F4500 fluorescence spectrophotometer. Samples were excited at 295 nm using a slit width of 5 nm, and emissions were recorded using a slit width of 5 nm from 295 to 410 nm. Samples were prepared with 2 μM YME1L-AAA+ in H150 reaction buffer [25 mM HEPES (pH 7.5) at 25 $^{\circ}\text{C}$, 150 mM NaCl, 10% glycerol] in the presence of either MANT-ATP, ATP or a mixture of ATP and Ribose. Working stock solutions for nucleotide samples were 750 μM and the ribose used was 2 mM. Samples were ran by increasing the concentration of the titrant until a volume of 0.3 mL of titrant (ATP or ATP and ribose mixture) had been added. Titrant was introduced into protein solution via 5-10 μL additions and allowed to reach equilibrium prior to collection of emissions spectra.

CHAPTER 3: RESULTS AND CONCLUSIONS

MANT-ATP Binds to More Than One Site on YME1L

The YME1LAAA+ domain was prepared by overexpression in *E. coli* and purified as described in Materials and Methods. Fluorescence titrations were run by titrating YME1L-AAA+ with MANT-ATP in various volumes until a total of 175 μ L of MANT-ATP was added. Unlike the other fluorescence experiments, the MANT spectra was analyzed between 310 and 500 nm to see the whole spectrum and avoid cutoff. Fluorescence data looks at FRET donor and acceptor properties, i.e. Tryptophan (Fluorescence intensity at 350 nm) and MANT (Fluorescence intensity at 450 nm) emissions (Figure 2). Figure 2A shows overall spectra with changing MANT-ATP signal out at 450 nm. The MANT-ATP signal increases as the concentration of MANT-ATP is increased. Figure 2B highlights the decreasing tryptophan signal as MANT-ATP concentration is increased, which is consistent with FRET.

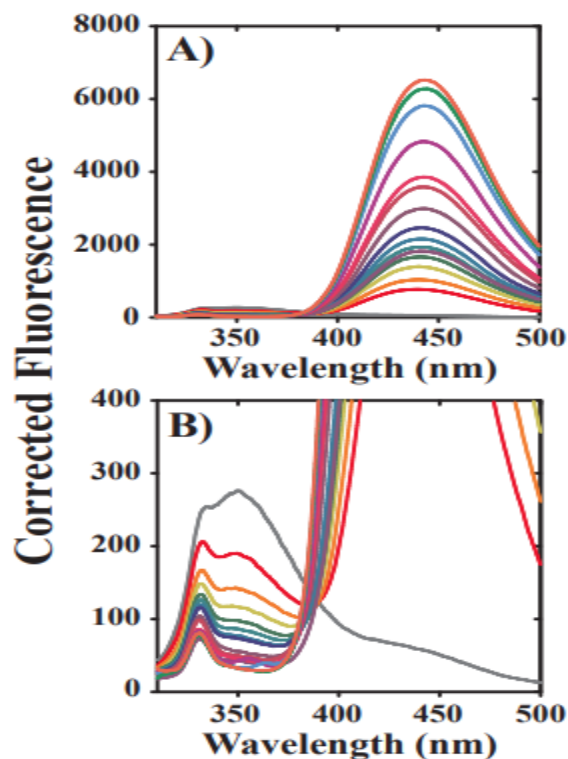


Figure 2. Representative MANT-ATP Binding Spectra. Panel A shows the overall spectrum of MANT-ATP. Panel B shows a close up view of the tryptophan signal and how that signal is depleted with increasing MANT-ATP volume. This is an example of the energy transfer between W518 and MANT-ATP.

The tryptophan signal (Figure 3, Panel A) displays a loss in signal with an estimated K_D equal to 3.2 ± 0.3 micromolar. The shape of the curve is a rectangular hyperbola, which is consistent with single-site binding. In Panel B of Figure 3, we see that the MANT emissions cannot be described by a single-site binding model as the tryptophan signal can. The data are not well described by a one-site binding model. Qualitative support for this is based on the lack of clear saturation behavior in the presence of MANT-ATP concentration up to 120 micromolar. Nonlinear least squares analyses indicate that the data are well described by a 2-site independent binding model. The first binding affinity, K_{D1} , is likely specific binding to the active site. The second binding affinity, K_{D2} , is likely nonspecific binding at other sites on the protein. In Panel C

of Figure 3, these data were fitted to a 2-site model, but the K_{D1} cannot accurately be estimated, hence the N.D. (Not Determined.) Experiments here were repeated in triplicate to validate the results. Values were obtained using the fractional saturation equation: $signal = A \times \frac{K[x]}{1+K[x]}$ where K is the equilibrium constant, A is the maximum amplitude (which we used a max value of 1), and [x] is the concentration of MANT-ATP. Fitting the data to a one-site model gave a curve that was not steep enough to fit the data, while a three-site model gave a curve that was too steep to fit the data.

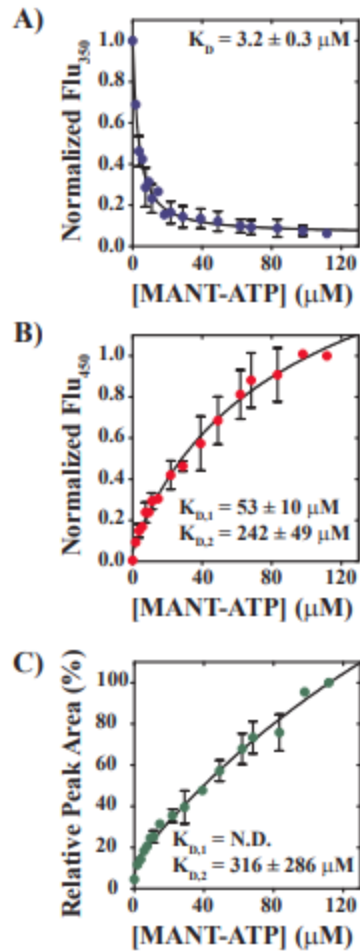


Figure 3. Resulting MANT-ATP Binding Parameters. Panel A shows tryptophan signal loss. Panel B shows MANT-ATP emissions fitted to a 2-site binding model. Panel C shows binding parameters as determined from relative peak area. K_{D1} could not accurately be determined.

ATP Binds Specifically to the Active Site

Fluorescence titrations were ran by titrating YME1L-AAA+ with ATP in various volumes until a total of 300 μL of ATP from a 750 micromolar stock solution was added. Tryptophan emissions spectra were collected by titrating non-fluorescent ATP into the AAA+ domain. This was motivated by the desire to determine whether the second binding site observed with MANT-ATP data is due to the MANT fluorophore being

present. The tryptophan spectra in Figure 4 shows a so-called quenching effect. Since ATP alone is not fluorescent, the way we can tell binding occurs is through the depletion of the tryptophan signal as the ATP concentration is increased. Experiments here were repeated in triplicate to validate results.

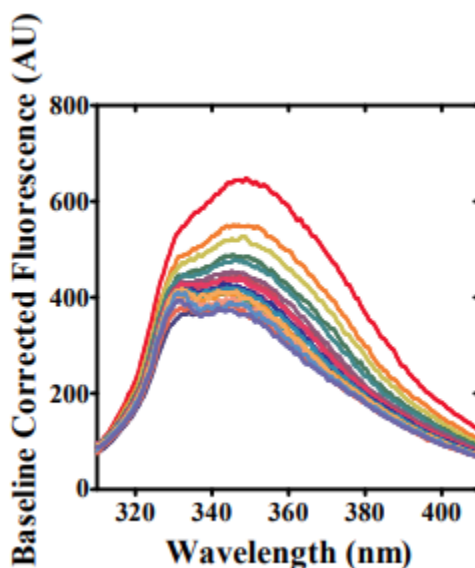


Figure 4. Representative Binding ATP Emissions Spectra. The figure shows the tryptophan signal being quenched as the ATP concentration was increased.

Fluorescence intensity and peak area analysis indicates a single binding site with affinities of 5.3 ± 0.6 micromolar, and 5.0 ± 0.6 micromolar, respectively. These data are similar to the first K_D from the MANT-ATP data (Figure 3A), thereby suggesting that K_{D2} from the MANT dataset is representative of nonspecific binding. The peak emissions wavelength in Panel C also shifts to a shorter wavelength, which is consistent with nucleotide binding shielding the W residue from bulk solvent interactions (Figure 5). The data were fitted to the fractional saturation equation listed above.

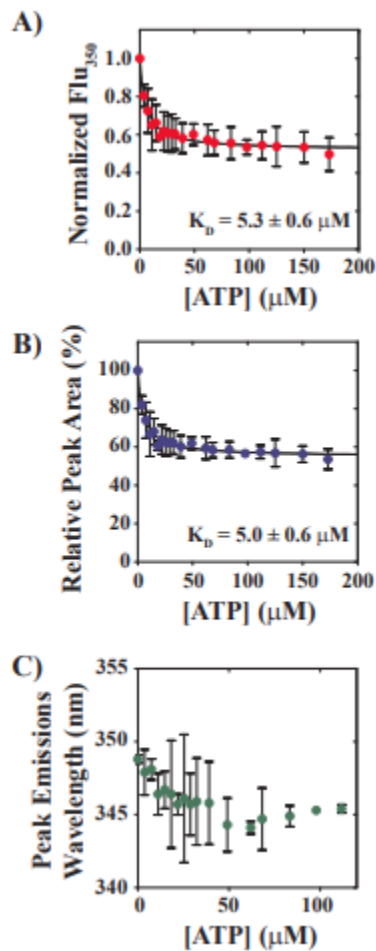


Figure 5. Resulting ATP Binding Parameters. Panel A shows the normalized fluorescence of tryptophan over increasing ATP concentrations. Panel B shows an estimated dissociation constant from the relative peak area, in percentage, over increasing concentrations of ATP. Panel C shows the shifting of the wavelength to an overall shorter wavelength over increasing ATP concentration.

Ribose acts as a competitor

Fluorescence titrations were ran by titrating YME1L-AAA+ with ATP, both in the presence of 2 mM ribose in various volumes until a total of 300 μL of ATP/Ribose was added. As indicated in Figure 5, the estimated K_D of ATP alone is around 5.3 ± 0.6 micromolar. From the fluorescence experiments with ATP in the presence of ribose, the K_D was then evaluated to be 245 ± 87 micromolar (Figure 6). Results were produced in triplicate to validate the results. This increase in K_D means that in the presence of ribose,

ATP has a much weaker attraction to the binding site of YME1L, meaning that ribose does act as a competitor, and it suggests that ribose can bind to the ATP binding site alone without the presence of adenine or the phosphates. To determine the equilibrium constant of ribose we fit the data to the fractional saturation equation but with an addition term to account for ribose. The equation used was $signal = A \times \frac{K[x]}{1+K[x]+K_y[y]}$ where K is the equilibrium constant of ATP determined from the previous experiment, [x] is the concentration of the ATP stock solution used, K_y is the equilibrium constant of ribose (what we were trying to determine), and [y] is the working concentration of ribose at 2mM.

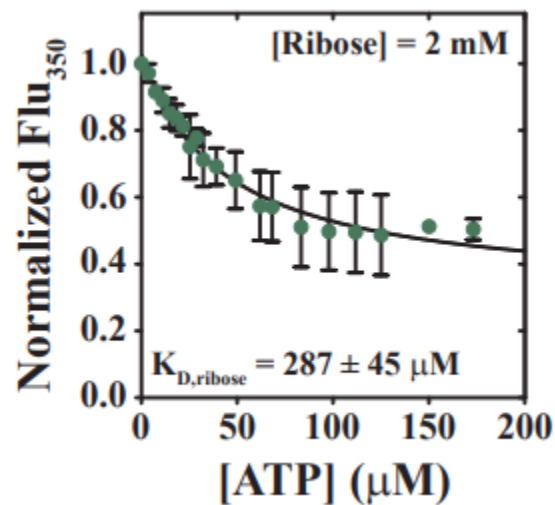


Figure 6. Representative Ribose Binding Spectra. Ribose fluorescence spectra over three trials. Shows dependence of fluorescence on ATP concentrations in the presence of 2mM ribose.

More work is still to be done in the future to test this observed result of ribose being a competitor of ATP. Control experiments need to be performed before fully validating this result. More work could be done to see if a K_{D1} can be accurately determined for MANT-ATP and its binding to other sites on the protein. There can also

be more work done to see if the other constituent of ATP, adenine, also plays a competitive roll in binding to YME1L. Once all the constituents of ATP are looked at in terms of binding affinity, the overall binding of ATP to the binding site on YME1L can be better understood as a sum of the individual nucleotide components. The overall goal in the long run is to obtain equilibrium constants of the individual nucleotide components and convert those values to Gibbs energy values, and see if the sum of these parts is equal to the overall Gibbs energy of ATP binding. The equation below gives a representation of the future goal of this experiment $\Delta G_{ATP} = \Delta G_{adenine} + \Delta G_{ribose} + \Delta G_{p_i}$.

WORKS CITED

- Brambley, Chad A, et al. "Characterization of Mitochondrial YME1L Protease Oxidative Stress-Induced Conformational State." *Journal of Molecular Biology* (2019): 1-16. Web. <https://doi.org/10.1016/j.jmb.2019.01.039>
- Mahoney, Diane E, et al. " Understanding D-Ribose and Mitochondrial Function." *Adv Biosci Clin Med* (2018): 1–5. Web. doi: 10.7575/aiac.abcm.v.6n.1p.1
- Miller, Justin M, et al. "Examination of the Role of Mg²⁺ in the Mechanism of Nucleotide Binding to the Monomeric YME1L AAA+ Domain." *Biochemistry* (2020): 1-15. Web. <https://dx.doi.org/10.1021/acs.biochem.0c00699>
- Osmanovic, Dino; Rabin, Yitzhak. "Effect of non-specific interactions on formation and stability of specific complexes." *The Journal of Chemical Physics* (2016): 1-2. Web. <https://doi.org/10.1063/1.4952981>
- Puchades, Cristina, et al. "Structure of the mitochondrial inner membrane AAA+ protease YME1 gives insight into substrate processing." *Structural Biology* (2017): 1-4. Web. doi: 10.1126/science.aao0464

APPENDIX A

Difference between initial and final runs of the ribose experiment. This shows the raw data of a similar quenching effect when the concentration of ATP is increased. Final run has the highest concentration of ATP. The spectrum was cut off at 350 nm due to an error in file export. The experiment was conducted between 310-410 nm but were only exported from 350 nm.

